

# Optical properties of $\text{UO}_2$ and $\text{PuO}_2$

Hongliang Shi,<sup>1,2</sup> Mingfu Chu,<sup>3</sup> and Ping Zhang<sup>1,4,\*</sup>

<sup>1</sup>*LCP, Institute of Applied Physics and Computational Mathematics,  
P.O. Box 8009, Beijing 100088, People's Republic of China*

<sup>2</sup>*SKLSM, Institute of Semiconductors, Chinese Academy of Sciences,  
P. O. Box 912, Beijing 100083, People's Republic of China*

<sup>3</sup>*State Key Laboratory for Surface Physics and Chemistry, Mianyang 621907, People's Republic of China*

<sup>4</sup>*Center for Applied Physics and Technology, Peking University, Beijing 100871, People's Republic of China*

We perform first-principles calculations of electronic structure and optical properties for  $\text{UO}_2$  and  $\text{PuO}_2$  based on the density functional theory using the generalized gradient approximation (GGA)+ $U$  scheme. The main features in orbital-resolved partial density of states for occupied  $f$  and  $p$  orbitals, unoccupied  $d$  orbitals, and related gaps are well reproduced compared to experimental observations. Based on the satisfactory ground-state electronic structure calculations, the dynamical dielectric function and related optical spectra, i.e., the reflectivity, adsorption coefficient, energy-loss, and refractive index spectrum, are obtained. These results are consistent well with the attainable experiments.

PACS numbers: 78.20.-e, 77.22.Ch, 71.20.-b

## I. INTRODUCTION

Actinide dioxides ( $\text{AnO}_2$ ) have been attracted lots of attention due to their rich physical phenomena characterized by the complex nature of  $5f$  electrons. Many experimental and theoretical works have been devoted to investigating the thermodynamical, electronic structural, and defect properties of  $\text{AnO}_2$  systems. Taking  $\text{UO}_2$  and  $\text{PuO}_2$  for example, their insulating ground states have been established experimentally [1, 2] and successfully predicted theoretically [3, 4, 5, 6]. When referring to insulators or semiconductors, one basic physical quantity of interest is their band gaps. If the band gap of  $\text{UO}_2$  or  $\text{PuO}_2$  can be comparable to semiconductors, one idea may occur to us that whether they can be applied extensively in the electronic and optoelectronic devices like semiconductors (Si, GaAs, and ZnO) or not. Recently, Meek *et al.* discussed the electronic properties of uranium dioxide and revealed the potential performance advantages of uranium dioxide as compared to conventional semiconductor materials [7]. Especially, the higher dielectric constant of  $\text{UO}_2$  makes it more suitable for making integrated circuits [7]. This may stimulate many studies of the optical properties for actinide dioxides in future.

Optical adsorption and reflectance spectra of semiconductors have been studied for several decades both experimentally and theoretically, whereas, similar works performed on actinide dioxides is still very scarce although they are necessary not only from the viewpoint of basic science but also from their technological importance in industries. Experimentally, Schoenes studied the incidence reflectivity of  $\text{UO}_2$  single crystals in the photon

energy range of 0.03-13 eV, from which the complex dielectric function  $\varepsilon(\omega) = \varepsilon_1(\omega) + i\varepsilon_2(\omega)$  has been derived [8]. For  $\text{PuO}_2$ , to our knowledge, no experimental optical data are available in literature. As for the theoretical investigations of optical spectrum of actinide dioxides, it is a great challenge to standard density functional theory that an accurate description of electronic structure for actinide oxides is hard to be achieved, which is indispensable to getting the correct optical spectrum. Conventional density functional schemes that apply the local density approximation (LDA) or the GGA underestimate the strong on-site Coulomb repulsion of the  $5f$  electrons and consequently fail to capture the correlation-driven localization. Therefore, the  $5f$  electrons in actinide oxides require special attention. One promising way to improve contemporary LDA and GGA approaches is to modify the intra-atomic Coulomb interaction through the so-called LDA+ $U$  or GGA+ $U$  approach, in which the underestimation of the intraband Coulomb interaction is corrected by the Hubbard  $U$  parameter [9, 10]. Recently, the electronic structures of  $\text{UO}_2$  and  $\text{PuO}_2$  are correctly reproduced using LDA+ $U$  or GGA+ $U$  calculations [3, 4, 5, 6]. Therefore, based on the good performance of LDA/GGA+ $U$  approaches in describing the electronic structure of the systems containing  $5f$  electrons, it is encouraging to investigate the optical spectra of them.

In this work, we used the GGA+ $U$  scheme to study the static and frequency-dependent dynamical dielectric response functions for  $\text{UO}_2$  and  $\text{PuO}_2$ . Our present calculated band gap  $E_g$  and high-frequency dielectric constant  $\varepsilon_\infty$  for  $\text{UO}_2$  are 2.3 eV and 5.53, which are in good agreement with the experimental values of about 2.1 eV and 5.1 observed in the optical spectra [8], respectively. Furthermore, our calculated dielectric function  $\varepsilon(\omega)$  exhibits the overall agreement with experimental result and the main peaks are well reproduced. The dielectric function and the consequent optical spectra for  $\text{PuO}_2$  are also

---

\*Author to whom correspondence should be addressed. Electronic address: zhang\_ping@iapcm.ac.cn

calculated in the paper. In particular, the value of  $\varepsilon_\infty$  for  $\text{PuO}_2$  is predicted to be 6.21, a little larger than that for  $\text{UO}_2$ . Considering the satisfactory calculations for  $\text{UO}_2$ , we expect our predicted optical behavior for  $\text{PuO}_2$  can provide a useful reference for future experimental measurement.

## II. DETAILS OF CALCULATION

Our electronic structural and optical calculations are performed using the projector-augmented wave (PAW) method of Blöchl [11], as implemented in the *ab initio* total-energy and molecular-dynamics program VASP (Vienna *ab initio* simulation program) [12]. PAW is an all-electron method that combines the accuracy of augmented-plane-wave methods with the efficiency of the pseudopotential approach. The PAW method is implemented in VASP with the frozen-core approximation. The exchange-correlation functional is used GGA of Perdew-Burke-Ernzerhof (PBE) formalism [13]. The  $5f$ ,  $6s$ ,  $6p$ ,  $6d$  and  $7s$  electrons of U and Pu as well as the oxygen  $2s$  and  $2p$  electrons are explicitly treated as valence electrons. The electron wave function is expanded in plane waves up to a cutoff energy of 500 eV. For the Brillouin zone integration, the  $\Gamma$  centered  $6 \times 6 \times 6$  grid is adopted. 144 bands are used to get the dynamical dielectric function  $\varepsilon(\omega)$  and a good convergence can be achieved. In order to perform the antiferromagnetic (AFM) phase calculations, we used the unit cell containing 12 atoms. The strong on-site Coulomb repulsion among the localized  $5f$  electrons is described by using the formalism formulated by Dudarev *et al.* [14]. In this scheme, only the difference between the spherically averaged screened Coulomb energy  $U$  and the exchange energy  $J$  is important for the total LDA (GGA) energy functional. Thus, in the following we label them as one single effective parameter  $U$  for brevity. In our calculation, we use  $J=0.51$  and  $0.75$  eV for the exchange energies of U and Pu, respectively, and the effective Hubbard  $U$  are 4.0 and 3 eV, which are close to the values used in other previous work [4, 5].

As for the optical spectra calculations, we adopt two different methods to determine the macroscopic static dielectric constants using different approximations [15]. One method is using a summation over conduction band states and the other is using the linear response theory (density functional theory). For the latter, only the static ion-clamped dielectric matrix can be obtained and a summation over empty conduction band states is not required, whereas the former can calculate the frequency-dependent dynamic dielectric function after the electronic ground state has been obtained. The frequency-dependent imaginary part of the dielectric function is determined by a summation over empty states using the

following equation [15]:

$$\varepsilon_{\alpha\beta}^{(2)}(\omega) = \frac{4\pi^2 e^2}{\Omega} \lim_{q \rightarrow 0} \frac{1}{q^2} \sum_{c,v,\mathbf{k}} 2w_{\mathbf{k}} \delta(\varepsilon_{c\mathbf{k}} - \varepsilon_{v\mathbf{k}} - \omega) \times \langle u_{c\mathbf{k}+\mathbf{e}_\alpha\mathbf{q}} | u_{v\mathbf{k}} \rangle \langle u_{c\mathbf{k}+\mathbf{e}_\beta\mathbf{q}} | u_{v\mathbf{k}} \rangle^*, \quad (1)$$

where the indices  $c$  and  $v$  refer to conduction and valence band states respectively, and  $u_{c\mathbf{k}}$  is the cell periodic part of the wavefunctions at the  $k$ -point  $\mathbf{k}$ . The real part of the dielectric tensor is obtained by the usual Kramers-Kronig transformation

$$\varepsilon_{\alpha\beta}^{(1)}(\omega) = 1 + \frac{2}{\pi} P \int_0^\infty \frac{\varepsilon_{\alpha\beta}^{(2)}(\omega') \omega'}{\omega'^2 - \omega^2 + i\eta} d\omega', \quad (2)$$

where  $P$  denotes the principle value.

The main optical spectra, such as the reflectivity  $R(\omega)$ , adsorption coefficient  $I(\omega)$ , energy-loss spectrum  $L(\omega)$ , and refractive index  $n(\omega)$ , all can be obtained from the dynamical dielectric response functions  $\varepsilon(\omega)$ . The explicit expressions are given by

$$R(\omega) = \left| \frac{\sqrt{\varepsilon(\omega)} - 1}{\sqrt{\varepsilon(\omega)} + 1} \right|^2, \quad (3)$$

$$I(\omega) = (\sqrt{2})\omega \left[ \sqrt{\varepsilon_1(\omega)^2 + \varepsilon_2(\omega)^2} - \varepsilon_1(\omega) \right]^{1/2}, \quad (4)$$

$$L(\omega) = \varepsilon_2(\omega) / [\varepsilon_1(\omega)^2 + \varepsilon_2(\omega)^2], \quad (5)$$

and

$$n(\omega) = (1/\sqrt{2}) \left[ \sqrt{\varepsilon_1(\omega)^2 + \varepsilon_2(\omega)^2} + \varepsilon_1(\omega) \right]^{1/2}, \quad (6)$$

respectively.

## III. RESULTS AND DISCUSSIONS

### A. electronic structure and optical properties of $\text{UO}_2$

Since the optical spectra are directly calculated from interband transitions, an accurate description of the electronic structure is indispensable. The calculated orbital-resolved partial density of states (PDOS) for U  $5f$ , U  $6d$  and O  $2p$  are shown in Fig. 1(a). The Fermi level is set to be zero. It is clearly shown that the valence bands are mainly contributed by U  $5f$  and O  $2p$  orbitals. The peak near the Fermi level is mainly U  $5f$  with a little O  $2p$  contribution, which has been confirmed by the resonant photoemission[16]. The U  $5f$  valence band covers from 0 to  $-1.6$  eV, which is also consistent with the experimental observation that the occupied  $5f$  states in  $\text{UO}_2$

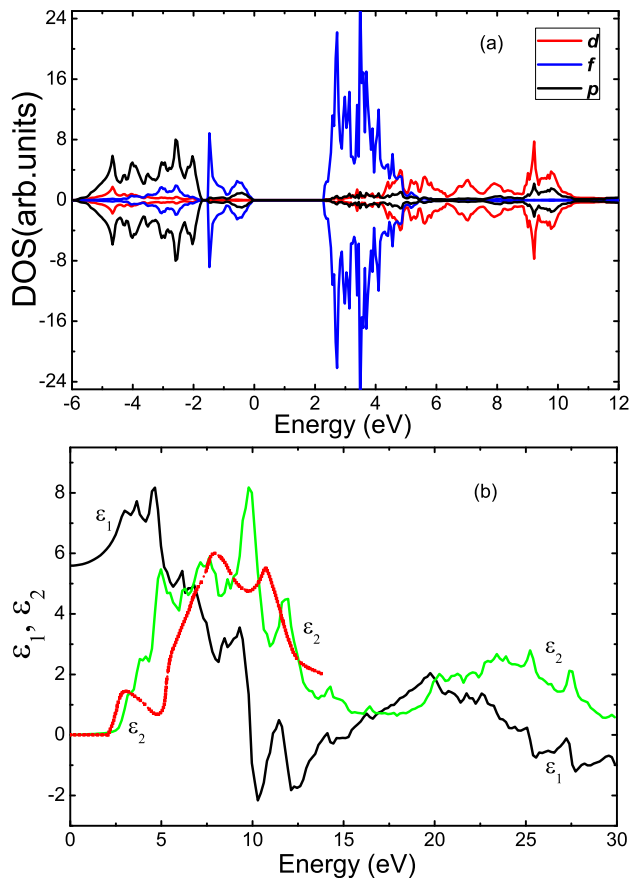


FIG. 1: (a) The projected orbital-resolved partial DOS for U  $6d$ , U  $5f$ , and O  $2p$  orbitals in antiferromagnetic  $\text{UO}_2$ . The Fermi level is set to zero. (b) The dynamical dielectric function  $\varepsilon(\omega) = \varepsilon_1(\omega) + i\varepsilon_2(\omega)$  as a function of the photon energy  $\omega$  for  $\text{UO}_2$ . The black and green lines represent our calculated real and imaginary parts of dielectric function  $\varepsilon(\omega)$ , respectively, while the red dotted-line is experimental  $\varepsilon_2(\omega)$ .

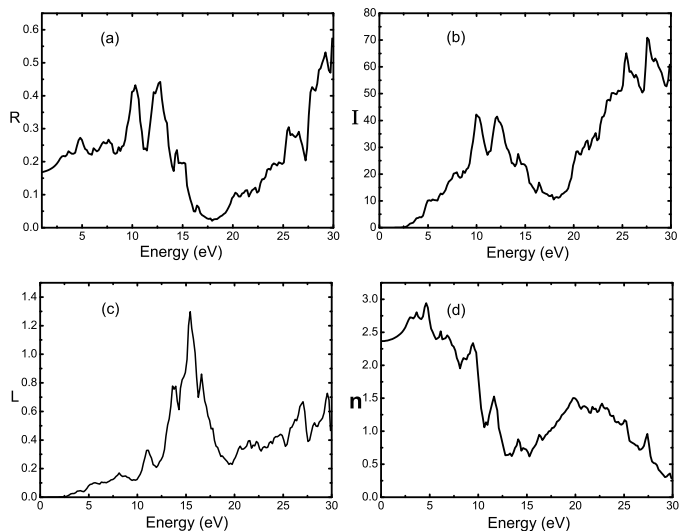


FIG. 2: Calculated optical spectra for  $\text{UO}_2$ , (a) the reflectivity  $R(\omega)$ , (b) adsorption coefficient  $I(\omega)$ , (c) energy-loss  $L(\omega)$ , and (d) refractive index  $n(\omega)$ .

TABLE I: Ion clamped static macroscopic dielectric constants  $\varepsilon_\infty$  of  $\text{UO}_2$  and  $\text{PuO}_2$  calculated using the PAW method and various approximations with various  $k$ -points sampling:  $\Gamma$  indicates a grid centered at  $\Gamma$  point, whereas Monkhorst-Pack (MP) grids do not contain the  $\Gamma$  point.  $N_k$  stands the number of irreducible  $k$ -points of the Brillouin zone (IBZ) at specific  $k$ -points sampling.  $\varepsilon_{\text{mic}}$  indicates values neglecting local field effects,  $\varepsilon_{\text{RPA}}$  includes local fields effects in the Hartree approximation, and  $\varepsilon_{\text{DFT}}$  includes local fields effects on the DFT level.  $\varepsilon^{\text{cond}}$  are values obtained by summation over conduction band states, whereas  $\varepsilon^{\text{LR}}$  are values obtained using linear response theory (density functional perturbation theory).

$\text{AnO}_2$	$k$ -mesh	$N_k$ (IBZ)	$\varepsilon_{\text{mic}}^{\text{LR}}$	$\varepsilon_{\text{RPA}}^{\text{LR}}$	$\varepsilon_{\text{DFT}}^{\text{LR}}$	$\varepsilon_{\text{mic}}^{\text{cond}}$
$\text{UO}_2$	$(12 \times 12 \times 12)\Gamma$	196	5.71	5.28	5.53	5.59
	$(8 \times 8 \times 8)\Gamma$	75	5.71	5.28	5.53	5.59
	$(6 \times 6 \times 6)\Gamma$	40	5.71	5.28	5.53	5.59
	$(6 \times 6 \times 6)\text{MP}$	18	5.71	5.28	5.53	5.59
$\text{PuO}_2$	$(12 \times 12 \times 12)\Gamma$	196	6.38	5.94	6.21	6.23
	$(8 \times 8 \times 8)\Gamma$	75	6.37	5.94	6.20	6.23
	$(6 \times 6 \times 6)\Gamma$	40	6.37	5.94	6.21	6.23
	$(6 \times 6 \times 6)\text{MP}$	18	6.37	5.94	6.20	6.23

are located around 1.5 eV below the Fermi level with a band width of about 2.0 eV [16]. The O  $2p$  valence band width is 4.0 eV from about  $-1.8$  to  $-5.8$  eV, in qualitative agreement with the photoemission value of 5.0 eV from  $-3.0$  to from  $-8.0$  eV [16].

As for the unoccupied U  $5f$  and  $6d$  orbitals, their accurate descriptions are also indispensable to the interband transitions, since electrons are excited from the occupied valence bands to the unoccupied bands during optical excitations. The  $5f$  and  $6d$  bands begin at about 2.3 and 4 eV, respectively, which are consistent well with the results of 2.6 and 5 eV obtained by hybrid DFT method [17]. Note that our calculated  $p \rightarrow d$  gap is 5.8 eV, which accords well with the Bremsstrahlung Isochromat Spectroscopy (BIS) value of  $5.0 \pm 0.4$  eV [18]. Overall, our calculated DOS agrees well the experimental spectra and other theoretical results. This supplies the safeguard for our following optical spectrum calculations.

Due to the cubic symmetry of  $\text{UO}_2$ , the dielectric tensor only has one independent component and  $\varepsilon_{xx} = \varepsilon_{yy} = \varepsilon_{zz}$ . Our calculated macroscopic dielectric constants  $\varepsilon_\infty$  using different methods and approximations are collected in Table I. We find that well converged results can be obtained by using the  $\Gamma$ -centered  $6 \times 6 \times 6$  grid. Note that the value of  $\varepsilon_{\text{DFT}}^{\text{LR}}$  should be compared to experiment. For  $\text{UO}_2$ , the calculated  $\varepsilon_\infty$  is 5.53, which agrees well with the experimental value of 5.1 [8].

As for the dynamical dielectric function, our calculated imaginary part  $\varepsilon_2(\omega)$  and real part  $\varepsilon_1(\omega)$  of the complex dielectric function  $\varepsilon(\omega)$  together with the corresponding experimental  $\varepsilon_2(\omega)$  are showed in Fig. 1(b). The green

and black lines represent our calculated imaginary and real parts of the complex dielectric function  $\varepsilon(\omega)$ , respectively, while the red dotted-line gives the experimental measurement [8] of  $\varepsilon_2(\omega)$ . Our theoretical photon energy covers from 0 to 30 eV, while the experimental [8] value covers from 0 to 13 eV. According to our calculated DOS showed in Fig. 1(a), we suggest that in  $\varepsilon_2(\omega)$  the peaks (at 2.8 eV) below 3 eV should be assigned to the intra  $5f$  transitions. Notice that the unoccupied  $6d$  bands begin about at 4 eV, therefore, the  $5f \rightarrow 6d$  transition energies should be larger than 4 eV. Kudin *et al.* also suggested that the stronger adsorption observed experimentally at  $\sim 5$ -6 eV could be assigned to the optically allowed  $5f \rightarrow 6d$  transitions [17]. According to our calculated  $\varepsilon_2(\omega)$ , four main peaks lie at about 5.0, 7.1, 9.8, and 11.8 eV, respectively. The shape of the calculated curve exhibits the same main features demonstrated by the experimental results [8]. Combined with the orbital-resolved PDOS shown in Fig. 1(a), we attribute the first two peaks in  $\varepsilon_2(\omega)$  to be  $5f \rightarrow 6d$  transitions, while the last two to be  $2p \rightarrow 6d$  transitions. This is consistent well with the experimental assignment [19] by Naegele *et al.*, who attributed the peak around 3 eV in  $\varepsilon_2(\omega)$  to intra  $5f^2$  transitions, while the peak structures above 5 and 10 eV were ascribed to the  $f \rightarrow d$  and  $p \rightarrow d$  transitions, respectively. Another assignment was suggested by Schoenes according to their dielectric function deduced from the reflectivity measurement; they argued that the peaks near 3 and 6 eV correspond to  $f \rightarrow d$  transitions, and that the peaks near 8 and 11 eV are due to  $p \rightarrow d$  transitions [8, 20]. Herein, the assignment of  $f \rightarrow d$  transition at 3 eV in Ref. [8, 20] is not supported by our calculation. The cause is that in assigning the peak in  $\varepsilon_2(\omega)$  at 3 eV, the energy distance between U occupied  $5f^2$  and O  $2p$  valence bands was overestimated in Ref. [8, 20] to be as large as 4 eV, which is much larger than that directly determined by the photoemission measurements [16, 21, 22]. On the contrary, according to our band-structure calculation, the occupied  $5f$  orbitals are locate at about 1.5 eV below the Fermi level and the O  $2p$  bands widely covers from about -1.8 to -5.8 eV, which instead accords well with the experimental photoemission data [16, 21, 22] in  $\text{UO}_2$ . Thus, as mentioned above, we suggest the structure in  $\varepsilon_2(\omega)$  below 3 eV is caused by the intra  $5f$  transitions.

Using expressions (3)-(7), the reflectivity  $R(\omega)$ , adsorption coefficient  $I(\omega)$ , energy-loss  $L(\omega)$  and refractive index  $n(\omega)$  spectra are showed in Fig. 2. For reflectivity  $R(\omega)$  spectrum, there are four peaks locating at 4.8, 7.6, 10.3, and 12.8 eV. The adsorption coefficient  $I(\omega)$  spectrum has the same trends. The origin of these peaks can also be explained as the peaks of the imaginary part  $\varepsilon_2(\omega)$ . Note that three similar peaks at 5.5, 8, 11.7 eV are also observed by the reflectance spectrum up to 13 eV at room temperature for  $\text{UO}_2$  [8]. The energy-loss  $L(\omega)$  spectrum can demonstrate not only one-particle excitations but also collective excitations. The maxima at around 15.4 eV as showed in Fig. 2(c) indicates the plas-

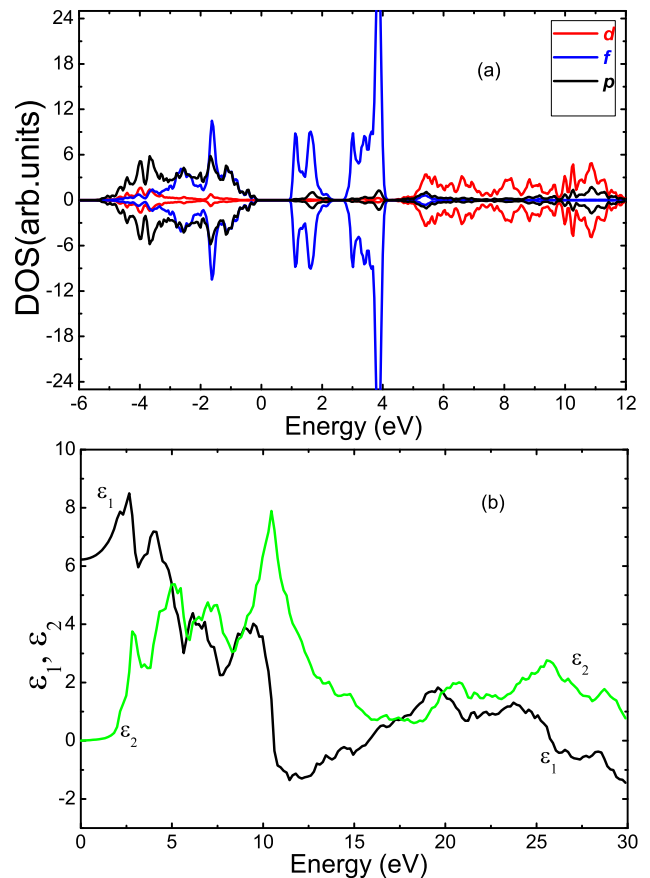


FIG. 3: (a) The projected orbital-resolved partial DOS for Pu  $6d$ , Pu  $5f$ , and O  $2p$  orbitals in antiferromagnetic  $\text{PuO}_2$ . The Fermi level is set to zero. (b) The dynamical dielectric function  $\varepsilon(\omega) = \varepsilon_1(\omega) + i\varepsilon_2(\omega)$  as a function of the photon energy  $\omega$  for  $\text{PuO}_2$ . The black and green lines represent our calculated real and imaginary parts of dielectric function  $\varepsilon(\omega)$ , respectively.

mon resonance, which is qualitatively consistent with the experimental value of 14 eV [20]. As showed in Fig. 1(b), at about 11.7 eV the real part  $\varepsilon_1$  becomes zero, arriving at the minima around 12.1 eV and then approaches zero at about 14 eV. As Schoenes pointed out, the energy at which  $\varepsilon_1(\omega)$  crosses the zero line with a positive slop gives the plasmon excitation energy [20].

## B. electronic structure and optical properties of $\text{PuO}_2$

Due to Pu unique position of its  $5f$  electrons between localized and delocalized states among actinide series, Pu metal and plutonium-based oxides have more complex properties than other actinides. For example, metallic Pu has six different phase under different temperatures and pressures [23].  $\text{PuO}_2$  as an important actinide dioxide has extensive applications in nuclear reactor fuel and long-term storage of surplus plutonium. Therefore, the

study of optical properties for  $\text{PuO}_2$  is also necessary and interesting. However, no experimental results of optical properties for  $\text{PuO}_2$  in literature are available. Recently, Butterfield *et al.* studied the photoemission behavior of surface oxides of  $\delta$ -plutonium and they observed that two peaks characterized by Pu  $5f$  and O  $2p$  orbitals are dominant in  $\text{PuO}_2$  and  $\text{Pu}_2\text{O}_3$  [24]. For  $\text{PuO}_2$ , the two peaks observed are located at approximately 2.5 and 4.6 eV [24], and our calculated DOS showed in Fig. 3(a) also present two similar peaks, i.e., a strong peak at about 1.6 eV and a weaker one at 3.7 eV. Overall, these features are well reflected in our PDOS showed in Fig. 3(a) compared to experimental observations. As for the unoccupied  $6d$  states, no experimental data can be obtained. Our calculated unoccupied  $6d$  states begin at about 5 eV. Considering the O  $2p$  peak at  $-3.7$  eV, we suggest the  $p \rightarrow d$  transitions occur at larger than 9 eV.

Our calculated macroscopic dielectric constant  $\epsilon_\infty$  for  $\text{PuO}_2$  are also collected in Table I. The present  $\epsilon_\infty$  is 6.21, whereas, no experimental value is unavailable at present. Our calculated imaginary part  $\epsilon_2(\omega)$  and real part  $\epsilon_1(\omega)$  of the complex dielectric function  $\epsilon(\omega)$  are showed in Fig. 3(b). For  $\epsilon_2(\omega)$ , four main peaks locate at 2.8, 5.1, 7.5, and 10.5 eV. According to our PDOS calculation showed in Fig. 3(a), we attribute the peak below 6 eV to be intra  $5f$  transitions, and the last two to be  $f \rightarrow d$  and  $p \rightarrow d$  transitions, respectively. The two similar peaks at 7 and 10 eV are also obtained by Jomard *et al.* using *ab initio* calculations [25].

Other related optical spectra for  $\text{PuO}_2$  are showed in Fig. 4. For reflectivity  $R(\omega)$  spectrum, there are four peaks at 2.8, 5.0, 7.5, and 10.6 eV. Similarly, four peaks at 3.0, 5.5, 7.6, 10.6 eV are also observed in the adsorption coefficient  $I(\omega)$  spectrum. The origin of these peaks can also be explained according to the structure displayed in the imaginary part  $\epsilon_2(\omega)$  of the dielectric function. It is evident that the plasmon excitation occurs at 16.0 eV, which is similar to the case of  $\text{UO}_2$  at 15.4 eV as mentioned above.

#### IV. SUMMARY

In summary, we have performed a detailed investigation of the electronic structure and optical spectra of actinide dioxides  $\text{UO}_2$  and  $\text{PuO}_2$  using first-principle methods. For  $\text{UO}_2$ , our calculated projected orbital-resolved PDOS for U  $5f$  and O  $2p$  orbitals in the valence region agree well with the experimental photoemission observation. As for the unoccupied states, our calculated  $p$ - $d$

gap is 5.8 eV, similar to the experimental BIS value of  $5.0 \pm 0.4$  eV. The calculated insulating band gap  $E_g$  and macroscopic static dielectric constants  $\epsilon_\infty$  for  $\text{UO}_2$  are 2.3 eV and 5.53, respectively, which are also in good agreement with the experimental values of about 2.1 eV and 5.1. The main features in spectra for  $\text{UO}_2$  are also well reproduced by our calculated dynamical dielectric function  $\epsilon(\omega)$  compared to the experimental observation. For

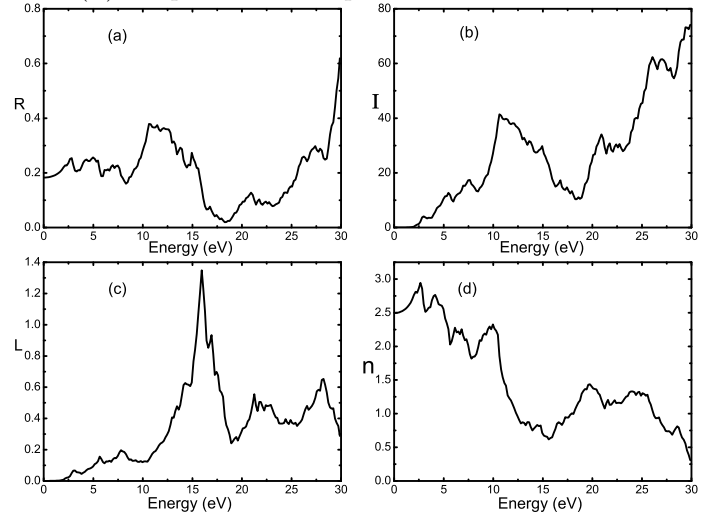


FIG. 4: Calculated optical spectra for  $\text{PuO}_2$ , (a) the reflectivity  $R(\omega)$ , (b) adsorption coefficient  $I(\omega)$ , (c) energy-loss  $L(\omega)$ , and (d) refractive index  $n(\omega)$ .

$\text{PuO}_2$ , the two main peaks characterized by Pu  $5f$  and O  $2p$  orbitals in valence bands are evidenced in our calculated PDOS, which accords well with the photoemission results. The calculated macroscopic static dielectric constants  $\epsilon_\infty$  is 6.21. The related optical spectra for  $\text{PuO}_2$  are also obtained by calculating the dynamical dielectric function. The  $f \rightarrow d$  and  $p \rightarrow d$  transitions are found to occur at 7.5 and 10.5 eV, respectively. Considering the satisfactory optical description for  $\text{UO}_2$  compared to experiments, we expect that these results for  $\text{PuO}_2$  are also reasonable and therefore can provide a useful reference for future experimental measurement.

#### Acknowledgments

This work was supported by the Foundations for Development of Science and Technology of China Academy of Engineering Physics under Grant No. 2009B0301037.

- 
- [1] J. Faber, Jr., G. H. Lander, and B. R. Cooper, Phys. Rev. Lett. **35** 1770 (1975).  
 [2] C. E. McNeilly, J. Nucl. Mater. **11**, 53 (1964).  
 [3] H. Geng, Y. Chen, Y. Kaneta, and M. Kinoshita, Phys. Rev. B **77**, 180101 (2008).

- [4] B. Sun, P. Zhang, and X.-G. Zhao, J. Chem. Phys. **128**, 084705 (2008).  
 [5] D. A. Andersson, J. Lezama, B. P. Uberuaga, C. Deo, and S. D. Conradson, Phys. Rev. B **79**, 024110 (2009).  
 [6] L. Petit, A. Svane, Z. Szotek, W. M. Temmerman, and

- G. M. Stocks, arXiv:0908.1806v1
- [7] T. Meek, M. Hu, and M. Haire, <http://www.nuenergy.org/pdf/UO2semicond.pdf>
- [8] J. Schoenes, *J. Appl. Phys.* **49**, 1463 (1978).
- [9] V.I. Anisimov, I.V. Solovyev, M.A. Korotin, M.T. Czyżyk, and G.A. Sawatzky, *Phys. Rev. B* **48**, 16929 (1993).
- [10] I.V. Solovyev, P.H. Dederichs, and V.I. Anisimov, *Phys. Rev. B* **50**, 16861 (1994).
- [11] P.E.Blöchl, *Phys. Rev. B* **50**, 17953 (1994).
- [12] G. Kresse and J. Hafner, *Phys. Rev. B* **48**, 13115 (1993).
- [13] J. P. Perdew, K. Burke, and M. Ernzerhof, *Phys. Rev. Lett.* **77**, 3865 (1996).
- [14] S. L. Dudarev, G. A. Botton, S. Y. Savrasov, C. J. Humphreys, and A. P. Sutton, *Phys. Rev. B* **57**, 1505 (1998).
- [15] M. Gajdoš, K. Hummer, G. Kresse, J. Furthmüller, and F. Bechstedt, *Phys. Rev. B* **73**, 045112 (2006).
- [16] L. E. Cox, W. P. Ellis, R. D. Cowan, J.W. Allen, S.-J. Oh, I. Lindau, B. B. Pate, and A. J. Arko, *Phys. Rev. B* **35**, 5761 (1987).
- [17] K. N. Kudin, G. E. Scuseria, and R. L. Martin, *Phys. Rev. Lett.* **89**, 266402 (2002).
- [18] Y. Baer and J. Schoenes, *Solid State Commun.* **33**, 885 (1980).
- [19] J. Naegele, L. Manes and U. Birkholz, *Proc. 5th Int. Conf. Plutonium and other Actinides*, ed. H.Blank and R. Lidner (North-Holland, Amsterdam, 1976), p. 393.
- [20] J. Schoenes, *Phys. Rep.* **63**, 301 (1980).
- [21] J. Naegele, *J. de Phys. C4*, 169 (1979).
- [22] P.R. Norton, R.L. Tapping, D.K. Creber and W.J.L. Buyers, *Phys. Rev. B* **21**, 2572 (1980).
- [23] K. T. Moore and G. van der Laan, *Rev. Mod. Phys.* **81**, 235 (2009).
- [24] M. Butterfield, T. Durakiewicz, E. Guziewicz, J. Joyce, A. Arko, K. Graham, D. Moore, and L. Morales, *Surf. Sci.* **571**, 74 (2004).
- [25] G. Jomard, B. Amadon, F. Bottin, and M. Torrent, *Phys. Rev. B* **78**, 075125 (2008).